

GraspMolmo: Generalizable Task-Oriented Grasping via Large-Scale Synthetic Data Generation

Abhay Deshpande

PRIOR, Allen Institute for AI
abhayd@allenai.org

Yuquan Deng

PRIOR, Allen Institute for AI
yuquand@allenai.org

Arijit Ray

Boston University
arijitr@bu.edu

Jordi Salvador

PRIOR, Allen Institute for AI
jordis@allenai.org

Winson Han

PRIOR, Allen Institute for AI
winsonh@allenai.org

Jiafei Duan

University of Washington
duanj1@cs.washington.edu

Kuo-Hao Zeng

kuohaozeng@gmail.com

Yuke Zhu

University of Texas at Austin
yukez@cs.utexas.edu

Ranjay Krishna

PRIOR, Allen Institute for AI
ranjayk@allenai.org

Rose Hendrix

PRIOR, Allen Institute for AI
roseh@allenai.org

Abstract: We present GraspMolmo, a generalizable open-vocabulary task-oriented grasping (TOG) model. GraspMolmo predicts semantically appropriate, stable grasps conditioned on a natural language instruction and a single RGB-D frame. For instance, given “pour me some tea,” GraspMolmo selects a grasp on a teapot handle rather than its body. Unlike prior TOG methods, which are limited by small datasets, simplistic language, and uncluttered scenes, GraspMolmo learns from PRISM, a novel large-scale synthetic dataset of 379k samples featuring cluttered environments and diverse, realistic task descriptions. We fine-tune the Molmo visual-language model on this data, enabling GraspMolmo to generalize to novel open-vocabulary instructions and objects. In challenging real-world evaluations, GraspMolmo achieves state-of-the-art results, with a 70% prediction success on complex tasks, compared to the 35% achieved by the next best alternative. GraspMolmo also successfully demonstrates the ability to predict semantically correct bimanual grasps zero-shot. We release our synthetic dataset, code, model, and benchmarks to accelerate research in task-semantic robotic manipulation, which, along with videos, are available at [this URL](#).

Keywords: Robots, Learning, Task-Oriented Grasping, Manipulation

1 Introduction

Robotic grasping has come a long way, with models now capable of robustly predicting stable grasps for a wide range of objects. Yet most existing methods operate in an object-centric fashion: they predict grasps that are stable for a given object but oblivious to the task at hand. In the real-world, however, how an object should be grasped depends crucially on what the robot is trying to do with it.

Consider a kitchen knife. A task-agnostic grasping system might simply choose a stable grasp anywhere on the knife, including the blade. While the blade might be an appropriate grasp site when

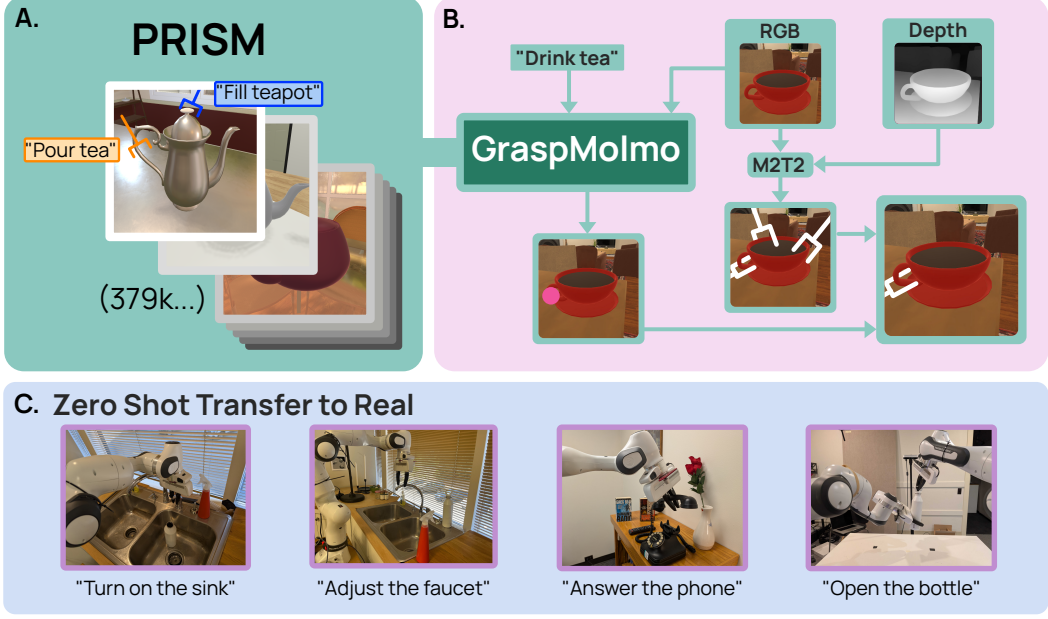


Figure 1: **A.** We introduce a large dataset of task-semantic-annotated tasks in virtual scenes with a large variety of target objects, which we name Purpose-driven Robotic Interaction in Scene Manipulation. **B.** We use PRISM to train GraspMolmo, which represents grasps as points and matches them to grasp proposals. **C.** We show strong transfer and generalization in real-world complex scenes with interesting task semantics using a 7-DoF Franka FR2 arm, and additionally show zero-shot adaptation to semantically-appropriate bimanual grasping.

handing the knife safely to another person, it would be ineffective for the purposes of chopping vegetables. These task-specific differences highlight the need for task-oriented grasping (TOG): The same physical object requires dramatically different grasps depending on the intended task [1, 2].

Recent work has introduced datasets and benchmarks [2, 3, 4], but they are limited in realism and diversity. Some contain relatively simple scenes without clutter and lack diverse object categories [2]. Others often template (e.g., “grasp the mug to pour” or “grasp the pan to clean”). These simplifications fail to capture the complexity of real-world environments and the wide variety of language humans use to specify tasks, such as “mince some garlic” or “do the dishes”. Furthermore, many models require pre-segmented point clouds [4] or multi-view observations [3], restricting real-time deployment.

To address these limitations, we propose GraspMolmo: a generalizable task-conditioned grasping model trained entirely on synthetic data. To overcome the brittleness of prior datasets, we create Purpose-driven Robotic Interaction in Scene Manipulation (or PRISM for short), a large-scale suite of task-grasp pairs with 10,000 scenes, 2,356 object instances, and task descriptions ranging from simple (“cut the apple”) to compositional or nuanced (“mince some garlic for a salad”). This dataset spans diverse cluttered scenes with realistic textures, occlusions, and multiple objects per task.

Using this dataset, we fine-tune Molmo [5], a recent open-weight vision-language model (VLM), to predict 6-DoF grasps from a single RGB-D frame and a task instruction. By grounding task semantics in the visual scene, GraspMolmo learns to disambiguate grasps that would otherwise be indistinguishable from a purely geometric perspective. GraspMolmo achieves state-of-the-art results on the TaskGrasp benchmark (76.7% versus the next best prior work at 72.3%). GraspMolmo also achieves significant performance boost on our benchmark of simulated cluttered scenes (62.5% versus 40.0%). Naturally, simulated evaluations are only a proxy, but we further demonstrate GraspMolmo transfers zero-shot to the real world in cluttered scenes, including objects and tasks completely unseen in training (70.4% prediction and 61.1% overall success rates). GraspMolmo also

zero-shot transfers to semantically-appropriate bimanual grasping in qualitative testing. We will release our dataset, model, code, and benchmarks to enable further research in task-semantic manipulation.

2 Related work

Task-oriented grasping. The field of Task-Oriented Grasping (TOG) addresses how robots should grasp objects based on intended tasks rather than just stability. Recent approaches have shown diverse strategies with specific limitations. GraspGPT [6] and FoundationGrasp [7] are most similar to our method, but due to their reliance on TaskGrasp, have limited pretraining with simple scenes and tasks. LERF-TOGO [8] uses language-embedded radiance fields to localize grasp points in a scene, but has costly requirements such as multiple views and long inference times, which make it impractical for use. RTAGrasp [9] transfers grasping behavior from human demonstrations but depends heavily on task-grounded data. Methods such as CROG and GraspCLIP [10, 11] represent a family of methods that perform inference directly on the image, outputting per-pixel predictions for grasp poses. These methods are limited to predicting only 4-DoF grasps, and strictly require a top-down camera view. TOGNet [12] extracts “patches of interest” in the image for grasping, but only accepts object-level rather than task-level grounding, resulting in coarse semantics that are ill-suited for diverse tasks. Underpinning many of these works, the TaskGrasp benchmark [13] provides evaluation standards and training data, but features simple scenes with limited task diversity. Our work addresses these collective limitations through comprehensive synthetic data generation with complex scenes, diverse and natural task specifications, and large data scale.

Vision-language models in robotics Recent years have witnessed significant progress in leveraging the strong vision-language commonsense capabilities of foundation multimodal language models (MLMs) [14, 15, 16, 17] for taking actions in the physical world [18, 19, 20, 21, 22]. Some studies employ pre-trained MLMs directly in a prompt-based manner [23, 24, 25, 26], while others further fine-tune or instruction-tune models for specific capabilities, including action policies [27, 19, 21, 28], physics [29], navigation [30, 31], and spatial reasoning [32, 33, 34]. Our approach aligns with the latter, fine-tuning a state-of-the-art MLM [15] on task descriptions and grounding points specifically for object grasping tasks. We advance beyond concurrent methods that separately address physics or multi-step reasoning limited to judging object relationships [33, 29] or precise pointing [32] without multi-step reasoning, by integrating both aspects (e.g., needing to reason about the precise point to grasp a pot to pour tea). In contrast to vision-language-action models that directly predict low-level controller actions [22, 21, 35], our method predicts grasp points in image space, enhancing generalizability and avoiding embodiment-specific constraints, thereby serving as a robust foundation model deployable across diverse hardware. While works like [31, 36, 32, 30] also predict points or high-level plans that are generalizable, they mainly focus on navigation and pick-and-place, while we focus on precise object manipulation, which is more difficult [36]. We also take inspiration from concurrent works [33, 37, 31] that show simulations as a scalable data source for real-world generalization. However, we generate large-scale, task-oriented grasping data that focuses on complex task-dependent object manipulation that goes beyond simpler QA or navigation tasks in these works.

Object affordances in robotics. Affordances describe the functional properties of objects—how they can be manipulated—linking perception to action beyond appearance. Affordance prediction has driven advances in learning-based 6-DoF grasping [38, 13, 39] and stable object placement [40, 41, 42, 32]. Researchers have explored various representations, including part-level segmentation [43], dense visual descriptors [44], and keypoint-based encodings [45, 46, 47]. At the policy level, affordances are often learned implicitly from demonstrations and generalized using rich visual features, as seen in TransporterNet [40], CLIPort [48], and recent works leveraging vision-language models (VLMs). However, many of these approaches rely on pretrained VLMs for visual grounding without incorporating deeper semantic reasoning, often resulting in less accurate or unstable point detection. In contrast, our approach instruction-tunes Molmo, a VLM enhanced for semantic understanding, to generate task-aware, stable grasp points through contextualized spatial reasoning.

3 Method

An overview of our overall method is presented in Fig. 1. First, we generate a large dataset of synthetic scenes with task-semantic-annotated tasks for each scene object. We then fine-tune a VLM by representing these grasps as points on the image, and then at inference time re-match these points to outputs from a grasp proposal network. An overview of the data generation process for PRISM-Train and PRISM-Test is presented in Fig. 2 and Sec. 3.1.

3.1 Generation of PRISM-Train and PRISM-Test

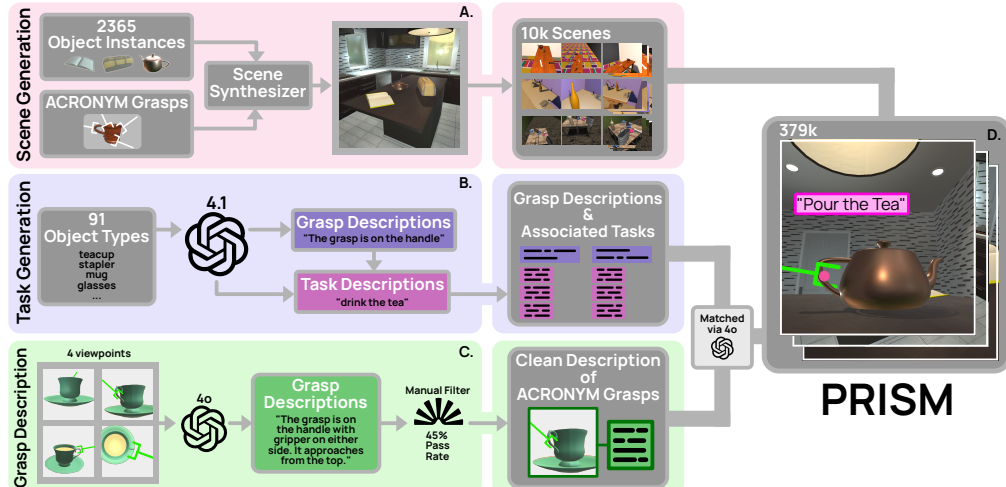


Figure 2: A major contribution is our generated dataset PRISM-Train and evaluation benchmark PRISM-Test (Sec. 3.1). First, synthetic scenes are generated from Shapenet-Sem [49] assets and ACRONYM [50] grasps. Next, object-centric spatial descriptions of grasps are generated and manually filtered and interesting and varied tasks are generated for object categories.

Scene Generation Our dataset employs assets from ShapeNet-Sem [49, 51] with grasps derived from ACRONYM [50]. We selected 91 object classes for use in data generation, enumerated in the supplement. Scene composition was performed using SceneSynthesizer [52], which allows for procedural generation of realistic object arrangements. We implemented additional lighting variations and camera randomization to increase the visual diversity of the training examples. As illustrated in Figure 2, we generated a comprehensive collection of diverse scenes spanning different object categories, lighting conditions, and spatial arrangements. Each scene was rendered from 10 distinct camera viewpoints to ensure robust training data that captures objects from multiple perspectives. This multi-view approach is particularly important, as grasp affordances often depend on the viewpoint, which can vary wildly in the real world. In our processing pipeline, we carefully track grasp visibility and only include grasps that are clearly visible in the specific renders for later stages of the learning process, ensuring that our model learns only from valid examples.

Grasp Descriptions as a Bridge Generating diverse task-grasp annotations at large scale is intractable, largely due to combinatorics, as every task-object-grasp triple must be annotated. In other words, annotating G grasps per object for O objects across T tasks is $\mathcal{O}(TOG)$. Our insight is that we can drastically reduce the effort required to generate task-grasp annotations by exploiting common structure. Namely, we note that many different tasks might require grasping an object in the same way. Concretely, pouring from a mug and drinking from it both require grasping the handle in the same manner. Therefore, we use *grasp descriptions* as the bridge between tasks and grasps. Instead of individually annotating each task-object-grasp triple with a binary label, we annotate each object-grasp pair with a natural language description of how the grasp is gripping the object. Separately, for each task we generate descriptions of how an object should be grasped to complete

that task. Then, matching tasks to object-grasp pairs reduces to simple text matching. The use of common-sense reasoning and natural language make this task well-suited for automation via LLMs, further aiding in scalability. The use of grasp descriptions decouples tasks from object-grasps pairs, meaning generating annotations is now $\mathcal{O}(T+OG)$, which is significantly more tractable to perform at large scale.

Grasp Description Generation For generating high-quality grasp descriptions, we employed a two-stage approach combining LLMs with human verification. Initially, we used GPT-4o [53] to generate synthetic grasp descriptions. To provide comprehensive visual context for the language model, we created collages containing four different viewpoints of each grasp scenario, enabling the model to consider the full 3D spatial relationship between the gripper and target object, with a sample shown in Fig. 2. To ensure description accuracy and quality, we then engaged human workers through the Prolific platform to verify each description, and provide corrections if necessary. We found that 45% of the synthetically generated grasp descriptions were judged to be accurate while the other 55% required correction, illustrating the importance of human verification for high quality data. Workers were instructed to identify and correct any inaccuracies in the AI-generated descriptions, particularly focusing on spatial relationships, contact points, and approach vectors. This human-in-the-loop verification process significantly improved the precision and natural language quality of our grasp descriptions, creating a dataset that balances the scalability of AI generation with the accuracy of human judgment.

Task Generation The process to generate semantic grasping tasks, leveraging the available knowledge in GPT-4.1 for a varied and rich set of instructions, involves two steps. Given an object class, we first prompt the LLM to generate two grasp descriptions that are maximally different while remaining plausible for manipulation tasks and avoiding hallucinating features which may or may not exist for an object of the given class. Then, we ask the LLM to generate four valid semantic tasks per grasp while minimizing compatibility of the instruction with the alternative grasp. In total, we generate 728 unique instructions corresponding to two grasps for each of the 91 object classes. For the complete prompts used to generate grasps and task instructions, please refer to the supplement.

Matching Tasks to Grasps Finally, we can match the generated grasp descriptions for each object-grasp pair with that of the generated tasks, which we accomplish using GPT-4o. Concretely, for each object in a scene we first determine the visible grasps, and corresponding grasp descriptions. For each generated task for that object, we then take the corresponding proposed grasp description and ask GPT-4o to determine which annotated object-grasp pair, if any, describes the same grasp. If the LLM determines that one of the existing grasps in the scene is described by the generated description, the task is paired with the object-grasp to create an task-object-grasp triple, and added to the dataset.

Assembling PRISM-Train and PRISM-Test To connect grasp data with visual perception, it becomes necessary to map ACRONYM grasps onto the image frame. To do this, we raycast from the grasp center onto the object being grasped, and project the resulting point onto the image plane. This process determines the pixel locations corresponding to each 3D grasp. PRISM-Train contains 9424 object-centric grasp instances across 2356 unique objects, which get scaled combinatorially via procedural generation. Although we do not use this information for training GraspMolmo , the dataset also includes calibrated 3D grasp poses for all objects, providing ground truth spatial information that can be used for both 2D and 3D perception tasks. The final dataset is 378,844 samples, each of which has a scene render, a task in natural language, a ground-truth semantically appropriate and stable grasp in calibrated camera coordinates, an object-centric spatial description of that grasp in natural language, and a pixel location corresponding to the proper grasp for that task. We present sample generated scenes from PRISM in Figure 4b, showcasing the diversity in objects, arrangements, and appearances.

3.2 TaskGrasp-Image

TaskGrasp [2] is a standard dataset in the field of task-oriented grasping, used for training and evaluation. The TaskGrasp dataset consists of partial object point clouds, each annotated with stable grasp poses. Each grasp on each object is annotated with binary labels, indicating whether each grasp satisfies a given task verb (e.g., scoop, cut, stir). However, the use of point clouds makes using image-based models difficult, especially due to limitations in the data such as noisy point cloud reconstructions caused by self-occlusions and segmentation artifacts. Additionally, the use of single verbs and nouns to define a task results in simplistic task conditioning, which insufficiently captures the richness of real-world human instructions.

To address these challenges, we construct TaskGrasp-Image, a new image-based dataset derived from the existing TaskGrasp dataset. Since TaskGrasp fuses multiple RGB-D views to create a single point cloud, we can perform inference on the images themselves instead of the point cloud, which is more suitable for image-based models, and is more realistic due to the absence of fusion, filtering, or segmentation artifacts. As a result, TaskGrasp-Image preserves the ground-truth grasp annotations while placing them in the context of real, unprocessed RGB-D imagery. We defer complete details on deriving TaskGrasp-Image from TaskGrasp to Section A.6.

3.3 GraspMolmo

Training Using PRISM-Train and the training data from TaskGrasp-Image (specifically, split 0 from the task split type), we create GraspMolmo by fine-tuning Molmo [15], a state-of-the-art VLM for pointing and spatial reasoning tasks, to point to grasps. We co-train on PixMo and all other Molmo training tasks in order to preserve the capability to generalize to unseen objects and settings while adapting to grasping. We use the natural language object-centric grasp description from our training data as a chain-of-thought processing step, requiring the model to output both the pixel location for the grasp and an object-centric description of that grasp. We sample 45% and 10% of our data mixture from PRISM-Train and TaskGrasp-Image, respectively, and proportionally downweight other data sources - please refer to supplemental materials for details on data mixture and hyperparameters.

Mapping Output Points to Grasps GraspMolmo outputs points on the image plane, which must be matched to a candidate grasp, predicted by a stable grasp generator, for output. To do so, we first map each grasp to a point on the image, by finding the point on the object being grasped (via closest-point queries), and projecting that point onto the image. We then output the grasp with the closest corresponding point to Molmo’s prediction. Concretely, given a set of candidate grasps $\mathcal{G} \subset \text{SE}(3)$, a function $f: \mathcal{G} \rightarrow \mathbb{R}^2$ that maps a grasp to a pixel coordinate, and the output $p \in \mathbb{R}^2$ from Molmo, we select the grasp $\hat{g} := \arg \min_{g \in \mathcal{G}} \|f(g) - p\|$.

4 Evaluation

We evaluate GraspMolmo and the most appropriate baseline on three distinct benchmark settings, progressively increasing in complexity and real-world applicability: a benchmark from literature with simple objects and minimal visual diversity, a synthetic held-out dataset of fully composed scenes with unseen objects, and finally, real-world transfer scenarios. The performance gap between methods widens notably as we progress from simpler to more complex evaluation scenarios, revealing fundamental differences in approach capabilities that are not apparent in basic benchmarks.

	TaskGrasp-Image	PRISM-Test	PRISM-Real (Prediction)	PRISM-Real (Overall)
Random	54.5%	29.3%	-	-
GraspGPT	72.3%	40.0%	35.1%	24.0%
Molmo	75.6%	49.8%	33.7%	31.0%
GraspMolmo	76.7%	62.5%	70.4%	61.1%

Table 1: Top-1 accuracy for grasp prediction across increasingly challenging task-oriented grasping settings. Following [6], we normalize across tasks for the TaskGrasp-Image evaluation. For real-world online evaluations, we separately report the prediction success rate (was the predicted grasp correct) and the overall success rate (was the predicted grasp correct *and* did the robot successfully grasp the object).

4.1 Baseline

We compare our method to GraspGPT [6], the current state-of-the-art approach in Task-Oriented Grasping, with similar assumptions to ours. We also compare to Molmo [5], which is simply the base VLM we fine-tune to create GraspMolmo, in order to illustrate the utility of training on PRISM. We follow previous works [13, 6, 7] in restricting real-world evaluations to single-view RGB-D observations, and in the interest of maximizing similarity with the real-world setting, we do the same for all evaluations.

We note that GraspGPT requires a segmented point cloud of the object, and therefore depends on Segment Anything 2 (SAM2) [54] and GroundingDINO [55] to extract the object point cloud for downstream processing. Additionally, in addition to the task instruction (e.g. “give me some water”), GraspGPT also requires access to the specific object being manipulated (e.g. water bottle), and the specific action primitive being performed (e.g. handover). In the real world, such extra information may not be available, limiting its applicability. For our experiments, we use GPT-4o to infer the specific object and task primitive from the task instruction and the image, which adds both computational overhead and the potential for error propagation. In contrast to these requirements, GraspMolmo directly processes raw sensor data and freeform natural language without needing intermediate segmentation or task simplification steps.

4.2 TaskGrasp-Image

For the TaskGrasp-Image benchmark, we follow the same data presentation format as detailed in Sec. 3.2 - single-view RGB-D observations rather than fused point clouds. We evaluate on split 0 of the “task” split type from TaskGrasp, and illustrate a performance increase over all baselines in Table 1.

4.3 PRISM-Test

PRISM-Test is a fully-synthetic evaluation set constructed using the same pipeline as our training data, but with both held-out object instances (of previously seen classes) and completely novel object classes composed into complete scenes. We defer full details, including a complete object list and randomization parameters, to Section A.1. This benchmark tests generalization capabilities across novel objects and novel scenes, while maintaining the controllable diversity and large scale of synthetic data. By evaluating on completely unseen object categories, we demonstrate that GraspMolmo learns generalizable task-grasp relationships rather than memorizing specific object-grasp pairings.

In these increasingly challenging scenarios with held-out objects and scenes, the performance differential between baselines widens. Table 1 shows our method achieves a 62.5% task-appropriate grasp success rate, while baselines drop to below 50%. This widening performance gap and lower success rates confirm our intuition that the complex scenes and tasks, along with diverse randomiza-

tion, make PRISM-Test a challenging and valuable benchmark. As illustrated in Figure 4a, we also see that PRISM-Test also correlates well with real-world performance, further proving its utility.

4.4 Real-World Transfer with PRISM-Real

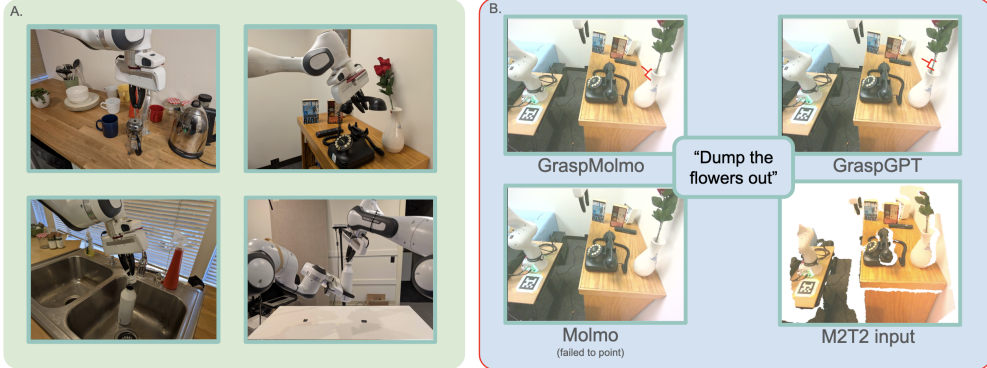


Figure 3: (a) We evaluate on three real-world scenes representative of in-home use cases, with varying objects with diverse task semantics. We also demonstrate zero-shot applicability to bimanual task-oriented grasping. (b) We illustrate sample grasp outputs from GraspMolmo and baselines for the task “dump the flowers out”, where the robot must grasp the vase and turn it over, to empty out the flowers. GraspMolmo correctly grasps the vase in an optimal position to flip it.

To demonstrate real-world transfer capabilities, we test on a real robot platform. We use M2T2 [42] as the stable grasp generator, and execute the predicted grasps on a 7-DoF Franka FR2 arm. We evaluate the considered methods on 3 realistic cluttered scenes, featuring a total of 9 household objects representative of in-home applications, each with 2 associated tasks. With 3 trials per task, we perform a total of 54 trials per method. For full details about the evaluation scenes, objects, and tasks, please refer to the supplement.

Since these evaluation scenes each contain multiple objects with meaningful variation in task semantics, we can evaluate both geometric grasp success and task appropriateness in realistic settings. This focus on objects with multiple affordances and associated tasks makes for a challenging evaluation, measuring a model’s ability to reason about how the semantics of a task inform grasping behavior, meaning simply memorizing task-agnostic object semantics is insufficient. Here, GraspMolmo outperforms baselines by a considerable margin as illustrated in Table 1, attaining a 70.4% accuracy for grasp predictions, more than double that of the closest baseline. We also report a 61.1% success rate overall, including execution on the robot, whereas the closest baseline attains 31%.

We will release this benchmark as an offline evaluation set to facilitate future research in task-oriented grasping. Figure 3 presents representative images from our real-world test scenes, showcasing the complexity and diversity of the evaluation environments.

4.5 Extension to bimanual grasping

While single-arm grasping has dominated robotic manipulation research, it faces inherent limitations for tasks requiring coordinated forces. Task-semantic bimanual grasping addresses these constraints by enabling opposing force application—essential for activities like unscrewing a water bottle cap, folding clothes, or lifting large objects. Our preliminary experiments in this area show that GraspMolmo preserves single-arm generalization capabilities while enabling task-semantic reasoning through prompt modifications. A qualitative sample may be seen in Fig.3A - while limited, this demonstrates that GraspMolmo supports new directions in robotic manipulation.

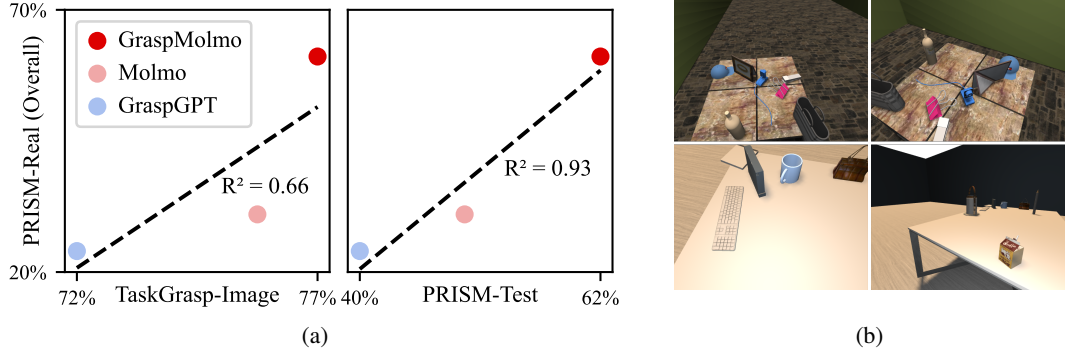


Figure 4: (a) Performance on PRISM-Test is a better indicator of success in real-world scenarios than TaskGrasp-Image. (b) Sample scenes and viewpoints, illustrating the object, viewpoint, and lighting diversity of PRISM.

5 Conclusion

Our work demonstrates significant advances in robotic grasping capabilities, with performance improvement on nontrivial task semantics and zero-shot generalization to cluttered real scenes. By developing a system that understands not just what an object is, but how it should be manipulated for specific intended uses, we aim to advance robotic manipulation beyond simple pick-and-place operations. Our approach demonstrates superior performance on realistic scenarios, successfully navigating cluttered environments and complex language instructions like “mince some garlic” rather than the constrained “grasp [noun] to [verb]” paradigm of previous work. The zero-shot generalization to real scenes validates our synthetic training methodology, while our zero-shot success with bimanual grasping showcases the flexibility of our task-semantic understanding. We will release GraspMolmo, PRISM-Train, PRISM-Test, and PRISM-Real, as well as our code for generating synthetic data to accelerate expansion in this direction. These contributions establish a new foundation for robotic manipulation by demonstrating a generalizable approach that functions effectively in cluttered environments while showing promising potential for zero-shot extension to bimanual tasks—a crucial step toward truly effective manipulation in unstructured real-world settings.

6 Limitations

Despite the advancements presented in this work, several limitations remain. Our approach still maintains a dependency on a grasp proposer, though it has successfully eliminated reliances on other auxiliary models such as SAM2, GroundingDINO, and GPT-4o. Additionally, GraspMolmo requires integration with motion planning algorithms or alternative policies to execute agent motion effectively. Furthermore, the point-based representation may prove inadequate for scenarios demanding fine-resolution rotational adjustments in grasping operations. Future research should focus on developing models capable of directly generating semantically-appropriate stable grasps without intermediate representations.

Acknowledgments

We thank our coworkers at PRIOR, particularly Rohun Tripathi, for helpful discussion and feedback.

References

- [1] R. Detry, J. Papon, and L. Matthies. Task-oriented grasping with semantic and geometric scene understanding. In *IEEE/RSJ Intl. Conf. on Intelligent Robots and Systems (IROS)*, 2017.
- [2] A. Murali, W. Liu, K. Marino, S. Chernova, and A. Gupta. Same object, different grasps: Data and semantic knowledge for task-oriented grasping. In *Conference on Robot Learning (CoRL)*, 2020.
- [3] K. Fang, Y. Zhu, A. Garg, A. Kurenkov, V. Mehta, L. Fei-Fei, and S. Savarese. Learning task-oriented grasping for tool manipulation from simulated self-supervision. In *Robotics: Science and Systems (RSS)*, 2018.
- [4] C. Tang, D. Huang, L. Meng, W. Liu, and H. Zhang. Task-oriented grasp prediction with visual-language inputs. In *IEEE/RSJ Intl. Conf. on Intelligent Robots and Systems (IROS)*, 2023.
- [5] M. Deitke, C. Clark, S. Lee, R. Tripathi, Y. Yang, and et al. Molmo and pixmo: Open weights and open data for state-of-the-art multimodal models. *arXiv preprint arXiv:2409.17146*, 2024.
- [6] C. Tang, D. Huang, W. Ge, W. Liu, and H. Zhang. Graspgrpt: Leveraging semantic knowledge from a large language model for task-oriented grasping. *IEEE Robotics and Automation Letters*, 8:7551–7558, 2023. URL <https://api.semanticscholar.org/CorpusId:260154903>.
- [7] C. Tang, W. Dong, R. Xu, H. Zhang, and D. Huang. Foundationgrasp: Generalizable task-oriented grasping with foundation models. *IEEE Transactions on Automation Science and Engineering*, 22:12418–12435, 2024. URL <https://api.semanticscholar.org/CorpusId:269157340>.
- [8] J. Kerr, C. M. Kim, K. Goldberg, L. Y. Chen, S. Sharma, A. Rashid, and A. Kanazawa. Language embedded radiance fields for zero-shot task-oriented grasping. In *Conference on Robot Learning*, 2023. URL <https://api.semanticscholar.org/CorpusId:261882332>.
- [9] W. Dong, D. Huang, J. Liu, C. Tang, and H. Zhang. Rtagrasp: Learning task-oriented grasping from human videos via retrieval, transfer, and alignment. *arXiv preprint arXiv:2409.16033*, 2024.
- [10] G. Tziasas, X. Yucheng, A. Goel, M. Kasaei, Z. Li, and H. Kasaei. Language-guided robot grasping: Clip-based referring grasp synthesis in clutter. In *7th Annual Conference on Robot Learning*, 2023.
- [11] C. Tang, D. Huang, L. Meng, W. Liu, and H. Zhang. Task-oriented grasp prediction with visual-language inputs. *2023 IEEE/RSJ International Conference on Intelligent Robots and Systems (IROS)*, pages 4881–4888, 2023. URL <http://ieeexplore.ieee.org/stamp/stamp.jsp?tp=&arnumber=10342268>.
- [12] P. Xie, S. Chen, D. Hu, Y. Dai, K. Yang, and G. Wang. Target-oriented object grasping via multimodal human guidance. *arXiv preprint arXiv:2408.11138*, 2024.
- [13] A. Murali, W. Liu, K. Marino, S. Chernova, and A. Gupta. Same object, different grasps: Data and semantic knowledge for task-oriented grasping. In *Conference on robot learning*, pages 1540–1557. PMLR, 2021.
- [14] H. Liu, C. Li, Q. Wu, and Y. J. Lee. Visual instruction tuning. In *NeurIPS*, 2023.
- [15] M. Deitke, C. Clark, S. Lee, R. Tripathi, Y. Yang, J. S. Park, M. Salehi, N. Muennighoff, K. Lo, L. Soldaini, J. Lu, T. Anderson, E. Bransom, K. Ehsani, H. Ngo, Y. Chen, A. Patel, M. Yatskar, C. Callison-Burch, A. Head, R. Hendrix, F. Bastani, E. VanderBilt, N. Lambert, Y. Chou,

- A. Chheda, J. Sparks, S. Skjonsberg, M. Schmitz, A. Sarnat, B. Bischoff, P. Walsh, C. Newell, P. Wolters, T. Gupta, K.-H. Zeng, J. Borchardt, D. Groeneveld, C. Nam, S. Lebrecht, C. Witlif, C. Schoenick, O. Michel, R. Krishna, L. Weihs, N. A. Smith, H. Hajishirzi, R. Girshick, A. Farhadi, and A. Kembhavi. Molmo and pixmo: Open weights and open data for state-of-the-art vision-language models, 2024. URL <https://arxiv.org/abs/2409.17146>.
- [16] J. Achiam, S. Adler, S. Agarwal, L. Ahmad, I. Akkaya, F. L. Aleman, D. Almeida, J. Altenschmidt, S. Altman, S. Anadkat, et al. Gpt-4 technical report. *arXiv preprint arXiv:2303.08774*, 2023.
- [17] M. Reid, N. Savinov, D. Teplyashin, D. Lepikhin, T. Lillicrap, J.-b. Alayrac, R. Soricut, A. Lazaridou, O. Firat, J. Schrittwieser, et al. Gemini 1.5: Unlocking multimodal understanding across millions of tokens of context. *arXiv preprint arXiv:2403.05530*, 2024.
- [18] B. Zitkovich, T. Yu, S. Xu, P. Xu, T. Xiao, F. Xia, J. Wu, P. Wohlhart, S. Welker, A. Wahid, Q. Vuong, V. Vanhoucke, H. T. Tran, R. Soricut, A. Singh, J. Singh, P. Sermanet, P. R. Sanketi, G. Salazar, M. S. Ryoo, K. Reymann, K. Rao, K. Pertsch, I. Mordatch, H. Michalewski, Y. Lu, S. Levine, L. Lee, T. E. Lee, I. Leal, Y. Kuang, D. Kalashnikov, R. Julian, N. J. Joshi, A. Irpan, B. Ichter, J. Hsu, A. Herzog, K. Hausman, K. Gopalakrishnan, C. Fu, P. Florence, C. Finn, K. A. Dubey, D. Driess, T. Ding, K. M. Choromanski, X. Chen, Y. Chebotar, J. Carabal, N. Brown, A. Brohan, M. G. Arenas, and K. Han. RT-2: vision-language-action models transfer web knowledge to robotic control. In J. Tan, M. Toussaint, and K. Darvish, editors, *Conference on Robot Learning, CoRL 2023, 6-9 November 2023, Atlanta, GA, USA*, volume 229 of *Proceedings of Machine Learning Research*, pages 2165–2183. PMLR, 2023. URL <https://proceedings.mlr.press/v229/zitkovich23a.html>.
- [19] M. J. Kim, K. Pertsch, S. Karamcheti, T. Xiao, A. Balakrishna, S. Nair, R. Rafailov, E. P. Foster, P. R. Sanketi, Q. Vuong, T. Kollar, B. Burchfiel, R. Tedrake, D. Sadigh, S. Levine, P. Liang, and C. Finn. Openvla: An open-source vision-language-action model. In P. Agrawal, O. Kroemer, and W. Burgard, editors, *Conference on Robot Learning, 6-9 November 2024, Munich, Germany*, volume 270 of *Proceedings of Machine Learning Research*, pages 2679–2713. PMLR, 2024. URL <https://proceedings.mlr.press/v270/kim25c.html>.
- [20] G. R. Team, S. Abeyruwan, J. Ainslie, J. Alayrac, M. G. Arenas, T. Armstrong, A. Balakrishna, R. Baruch, M. Bauzá, M. Blokzijl, S. Bohez, K. Bousmalis, A. Brohan, T. Buschmann, A. Byravan, S. Cabi, K. Caluwaerts, F. Casarini, O. Chang, J. E. Chen, X. Chen, H. L. Chiang, K. Choromanski, D. D'Ambrosio, S. Dasari, T. Davchev, C. Devin, N. D. Palo, T. Ding, A. Dostmohamed, D. Driess, Y. Du, D. Dwibedi, M. Elabd, C. Fantacci, C. Fong, E. Frey, C. Fu, M. Giustina, K. Gopalakrishnan, L. Graesser, L. Hasenclever, N. Heess, B. Hernaez, A. Herzog, R. A. Hofer, J. Humplik, A. Iscen, M. G. Jacob, D. Jain, R. Julian, D. Kalashnikov, M. E. Karagozler, S. Karp, J. C. Kew, J. Kirkland, S. Kirmani, Y. Kuang, T. Lampe, A. Laurens, I. Leal, A. X. Lee, T. E. Lee, J. Liang, Y. Lin, S. Maddineni, A. Majumdar, A. H. Michaely, R. Moreno, M. Neunert, F. Nori, C. Parada, E. Parisotto, P. Pastor, A. Pooley, K. Rao, K. Reymann, D. Sadigh, S. Saliceti, P. Sanketi, P. Sermanet, D. Shah, M. Sharma, K. Shea, C. Shu, V. Sindhwani, S. Singh, R. Soricut, J. T. Springenberg, R. Sterneck, R. Surdulescu, J. Tan, J. Tompson, V. Vanhoucke, J. Varley, G. Vesom, G. Vezzani, O. Vinyals, A. Wahid, and S. Welker. Gemini robotics: Bringing AI into the physical world. *CoRR*, abs/2503.20020, 2025. doi:10.48550/ARXIV.2503.20020. URL <https://doi.org/10.48550/arXiv.2503.20020>.
- [21] K. Black, N. Brown, D. Driess, A. Esmail, M. Equi, C. Finn, N. Fusai, L. Groom, K. Hausman, B. Ichter, S. Jakubczak, T. Jones, L. Ke, S. Levine, A. Li-Bell, M. Mothukuri, S. Nair, K. Pertsch, L. X. Shi, J. Tanner, Q. Vuong, A. Walling, H. Wang, and U. Zhilinsky. π_0 : A vision-language-action flow model for general robot control. *CoRR*, abs/2410.24164, 2024. doi:10.48550/ARXIV.2410.24164. URL <https://doi.org/10.48550/arXiv.2410.24164>.

- [22] J. Bjorck, F. Castañeda, N. Cherniadev, X. Da, R. Ding, Linxi, Y. Fang, D. Fox, F. Hu, S. Huang, J. Jang, Z. Jiang, J. Kautz, K. Kundalia, L. Lao, Z. Li, Z. Lin, K. Lin, G. Liu, E. LLontop, L. Magne, A. Mandlekar, A. Narayan, S. Nasiriany, S. Reed, Y. L. Tan, G. Wang, Z. Wang, J. Wang, Q. Wang, J. Xiang, Y. Xie, Y. Xu, Z. Xu, S. Ye, Z. Yu, A. Zhang, H. Zhang, Y. Zhao, R. Zheng, and Y. Zhu. GR00T N1: an open foundation model for generalist humanoid robots. *CoRR*, abs/2503.14734, 2025. doi:10.48550/ARXIV.2503.14734. URL <https://doi.org/10.48550/arXiv.2503.14734>.
- [23] F. Liu, K. Fang, P. Abbeel, and S. Levine. Moka: Open-vocabulary robotic manipulation through mark-based visual prompting. *arXiv preprint arXiv:2403.03174*, 2024.
- [24] H. Huang, F. Lin, Y. Hu, S. Wang, and Y. Gao. Copa: General robotic manipulation through spatial constraints of parts with foundation models. *arXiv preprint arXiv:2403.08248*, 2024.
- [25] W. Huang, C. Wang, Y. Li, R. Zhang, and L. Fei-Fei. Rekep: Spatio-temporal reasoning of relational keypoint constraints for robotic manipulation. *arXiv preprint arXiv:2409.01652*, 2024.
- [26] J. Duan, W. Yuan, W. Pumacay, Y. R. Wang, K. Ehsani, D. Fox, and R. Krishna. Manipulate-anything: Automating real-world robots using vision-language models. *arXiv preprint arXiv:2406.18915*, 2024.
- [27] X. Li, C. Mata, J. Park, K. Kahatapitiya, Y. S. Jang, J. Shang, K. Ranasinghe, R. Burgert, M. Cai, Y. J. Lee, et al. Llara: Supercharging robot learning data for vision-language policy. *arXiv preprint arXiv:2406.20095*, 2024.
- [28] J. Duan, W. Pumacay, N. Kumar, Y. R. Wang, S. Tian, W. Yuan, R. Krishna, D. Fox, A. Mandlekar, and Y. Guo. Aha: A vision-language-model for detecting and reasoning over failures in robotic manipulation. *arXiv preprint arXiv:2410.00371*, 2024.
- [29] W. Chow, J. Mao, B. Li, D. Seita, V. Guizilini, and Y. Wang. Physbench: Benchmarking and enhancing vision-language models for physical world understanding. *arXiv preprint arXiv:2501.16411*, 2025.
- [30] J. Zhang, Z. Huang, A. Ray, and E. Ohn-Bar. Feedback-guided autonomous driving. In *Proceedings of the IEEE/CVF Conference on Computer Vision and Pattern Recognition (CVPR)*, pages 15000–15011, June 2024.
- [31] K. Ehsani, T. Gupta, R. Hendrix, J. Salvador, L. Weihs, K.-H. Zeng, K. P. Singh, Y. Kim, W. Han, A. Herrasti, R. Krishna, D. Schwenk, E. VanderBilt, and A. Kembhavi. Spoc: Imitating shortest paths in simulation enables effective navigation and manipulation in the real world, 2024. URL <https://arxiv.org/abs/2312.02976>.
- [32] W. Yuan, J. Duan, V. Blukis, W. Pumacay, R. Krishna, A. Murali, A. Mousavian, and D. Fox. Robopoint: A vision-language model for spatial affordance prediction for robotics. *arXiv preprint arXiv:2406.10721*, 2024.
- [33] A. Ray, J. Duan, R. Tan, D. Bashkirova, R. Hendrix, K. Ehsani, A. Kembhavi, B. A. Plummer, R. Krishna, K.-H. Zeng, et al. Sat: Spatial aptitude training for multimodal language models. *arXiv preprint arXiv:2412.07755*, 2024.
- [34] C. H. Song, V. Blukis, J. Tremblay, S. Tyree, Y. Su, and S. Birchfield. Robospatial: Teaching spatial understanding to 2d and 3d vision-language models for robotics, 2025. URL <https://arxiv.org/abs/2411.16537>.
- [35] A. Brohan, N. Brown, J. Carbajal, Y. Chebotar, X. Chen, K. Choromanski, T. Ding, D. Driess, A. Dubey, C. Finn, et al. Rt-2: Vision-language-action models transfer web knowledge to robotic control. *arXiv preprint arXiv:2307.15818*, 2023.

- [36] K.-H. Zeng, Z. Zhang, K. Ehsani, R. Hendrix, J. Salvador, A. Herrasti, R. Girshick, A. Kembhavi, and L. Weihs. Poliformer: Scaling on-policy rl with transformers results in masterful navigators, 2024. URL <https://arxiv.org/abs/2406.20083>.
- [37] S. Silwal, K. Yadav, T. Wu, J. Vakil, A. Majumdar, S. Arnaud, C. Chen, V.-P. Berges, D. Batra, A. Rajeswaran, et al. What do we learn from a large-scale study of pre-trained visual representations in sim and real environments? In *2024 IEEE International Conference on Robotics and Automation (ICRA)*, pages 17515–17521. IEEE, 2024.
- [38] M. Sundermeyer, A. Mousavian, R. Triebel, and D. Fox. Contact-grasnet: Efficient 6-dof grasp generation in cluttered scenes. In *2021 IEEE International Conference on Robotics and Automation (ICRA)*, pages 13438–13444. IEEE, 2021.
- [39] Z. Jiang, Y. Zhu, M. Svetlik, K. Fang, and Y. Zhu. Synergies between affordance and geometry: 6-dof grasp detection via implicit representations. *Robotics: science and systems*, 2021.
- [40] A. Zeng, P. Florence, J. Tompson, S. Welker, J. Chien, M. Attarian, T. Armstrong, I. Krasin, D. Duong, V. Sindhwani, et al. Transporter networks: Rearranging the visual world for robotic manipulation. *Conference on Robot Learning*, 2020.
- [41] W. Liu, C. Paxton, T. Hermans, and D. Fox. Structformer: Learning spatial structure for language-guided semantic rearrangement of novel objects. In *2022 International Conference on Robotics and Automation (ICRA)*, pages 6322–6329. IEEE, 2022.
- [42] W. Yuan, A. Murali, A. Mousavian, and D. Fox. M2t2: Multi-task masked transformer for object-centric pick and place. *arXiv preprint arXiv:2311.00926*, 2023.
- [43] T.-T. Do, A. Nguyen, and I. Reid. Affordancenet: An end-to-end deep learning approach for object affordance detection. In *International Conference on Robotics and Automation (ICRA)*, 2018.
- [44] P. Florence, L. Manuelli, and R. Tedrake. Dense object nets: Learning dense visual object descriptors by and for robotic manipulation. *Conference on Robot Learning*, 2018.
- [45] L. Manuelli, W. Gao, P. Florence, and R. Tedrake. kpam: Keypoint affordances for category-level robotic manipulation. In *The International Symposium of Robotics Research*, pages 132–157. Springer, 2019.
- [46] Z. Qin, K. Fang, Y. Zhu, L. Fei-Fei, and S. Savarese. Keto: Learning keypoint representations for tool manipulation. In *2020 IEEE International Conference on Robotics and Automation (ICRA)*, pages 7278–7285. IEEE, 2020.
- [47] K. Mo, L. J. Guibas, M. Mukadam, A. Gupta, and S. Tulsiani. Where2act: From pixels to actions for articulated 3d objects. In *Proceedings of the IEEE/CVF International Conference on Computer Vision*, pages 6813–6823, 2021.
- [48] M. Shridhar, L. Manuelli, and D. Fox. Cliprot: What and where pathways for robotic manipulation. In *Conference on robot learning*, pages 894–906. PMLR, 2022.
- [49] A. X. Chang, T. Funkhouser, L. Guibas, P. Hanrahan, Q. Huang, Z. Li, S. Savarese, M. Savva, S. Song, H. Su, J. Xiao, L. Yi, and F. Yu. ShapeNet: An Information-Rich 3D Model Repository. Technical Report arXiv:1512.03012 [cs.GR], Stanford University — Princeton University — Toyota Technological Institute at Chicago, 2015.
- [50] C. Eppner, A. Mousavian, and D. Fox. Acronym: A large-scale grasp dataset based on simulation. In *2021 IEEE International Conference on Robotics and Automation (ICRA)*, pages 6222–6227, 2021. doi:10.1109/ICRA48506.2021.9560844.

- [51] M. Savva, A. X. Chang, and P. Hanrahan. Semantically-Enriched 3D Models for Commonsense Knowledge. *CVPR 2015 Workshop on Functionality, Physics, Intentionality and Causality*, 2015.
- [52] C. Eppner, A. Murali, C. Garrett, R. O’Flaherty, T. Hermans, W. Yang, and D. Fox. scene_synthesizer: A python library for procedural scene generation in robot manipulation. *Journal of Open Source Software*, 2024.
- [53] OpenAI, ;, A. Hurst, A. Lerer, A. P. Goucher, A. Perelman, A. Ramesh, A. Clark, A. Ostrow, A. Welihinda, A. Hayes, A. Radford, A. Madry, A. Baker-Whitcomb, A. Beutel, A. Borzunov, A. Carney, A. Chow, A. Kirillov, A. Nichol, A. Paino, A. Renzin, A. T. Passos, A. Kirillov, A. Christakis, A. Conneau, A. Kamali, A. Jabri, A. Moyer, A. Tam, A. Crookes, A. Tootoochian, A. Tootoonchian, A. Kumar, A. Vallone, A. Karpathy, A. Braunstein, A. Cann, A. Codispoti, A. Galu, A. Kondrich, A. Tulloch, A. Mishchenko, A. Baek, A. Jiang, A. Pelisse, A. Woodford, A. Gosalia, A. Dhar, A. Pantuliano, A. Nayak, A. Oliver, B. Zoph, B. Ghorbani, B. Leimberger, B. Rossen, B. Sokolowsky, B. Wang, B. Zweig, B. Hoover, B. Samic, B. McGrew, B. Spero, B. Giertler, B. Cheng, B. Lightcap, B. Walkin, B. Quinn, B. Guaraci, B. Hsu, B. Kellogg, B. Eastman, C. Lugaressi, C. Wainwright, C. Bassin, C. Hudson, C. Chu, C. Nelson, C. Li, C. J. Shern, C. Conger, C. Barette, C. Voss, C. Ding, C. Lu, C. Zhang, C. Beaumont, C. Hallacy, C. Koch, C. Gibson, C. Kim, C. Choi, C. McLeavey, C. Hesse, C. Fischer, C. Winter, C. Czarnecki, C. Jarvis, C. Wei, C. Koumouzelis, D. Sherburn, D. Kappler, D. Levin, D. Levy, D. Carr, D. Farhi, D. Mely, D. Robinson, D. Sasaki, D. Jin, D. Valladares, D. Tsipras, D. Li, D. P. Nguyen, D. Findlay, E. Oiwoh, E. Wong, E. Asdar, E. Proehl, E. Yang, E. Antonow, E. Kramer, E. Peterson, E. Sigler, E. Wallace, E. Brevdo, E. Mays, F. Khorasani, F. P. Such, F. Raso, F. Zhang, F. von Lohmann, F. Sulit, G. Goh, G. Oden, G. Salmon, G. Starace, G. Brockman, H. Salman, H. Bao, H. Hu, H. Wong, H. Wang, H. Schmidt, H. Whitney, H. Jun, H. Kirchner, H. P. de Oliveira Pinto, H. Ren, H. Chang, H. W. Chung, I. Kivlichan, I. O’Connell, I. O’Connell, I. Osband, I. Silber, I. Sohl, I. Okuyucu, I. Lan, I. Kostrikov, I. Sutskever, I. Kanitscheider, I. Gulrajani, J. Coxon, J. Menick, J. Pachocki, J. Aung, J. Betker, J. Crooks, J. Lennon, J. Kiros, J. Leike, J. Park, J. Kwon, J. Phang, J. Teplitz, J. Wei, J. Wolfe, J. Chen, J. Harris, J. Varavva, J. G. Lee, J. Shieh, J. Lin, J. Yu, J. Weng, J. Tang, J. Yu, J. Jang, J. Q. Candela, J. Beutler, J. Landers, J. Parish, J. Heidecke, J. Schulman, J. Lachman, J. McKay, J. Uesato, J. Ward, J. W. Kim, J. Huizinga, J. Sitkin, J. Kraaijeveld, J. Gross, J. Kaplan, J. Snyder, J. Achiam, J. Jiao, J. Lee, J. Zhuang, J. Harriman, K. Fricke, K. Hayashi, K. Singhal, K. Shi, K. Karthik, K. Wood, K. Rimbach, K. Hsu, K. Nguyen, K. Gu-Lemberg, K. Button, K. Liu, K. Howe, K. Muthukumar, K. Luther, L. Ahmad, L. Kai, L. Itow, L. Workman, L. Pathak, L. Chen, L. Jing, L. Guy, L. Fedus, L. Zhou, L. Mamitsuka, L. Weng, L. McCalum, L. Held, L. Ouyang, L. Feuvrier, L. Zhang, L. Kondraciuk, L. Kaiser, L. Hewitt, L. Metz, L. Doshi, M. Aflak, M. Simens, M. Boyd, M. Thompson, M. Dukhan, M. Chen, M. Gray, M. Hudnall, M. Zhang, M. Aljubeh, M. Litwin, M. Zeng, M. Johnson, M. Shetty, M. Gupta, M. Shah, M. Yatbaz, M. J. Yang, M. Zhong, M. Glaese, M. Chen, M. Janner, M. Lampe, M. Petrov, M. Wu, M. Wang, M. Fradin, M. Pokrass, M. Castro, M. O. T. de Castro, M. Pavlov, M. Brundage, M. Wang, M. Khan, M. Murati, M. Bavarian, M. Lin, M. Yesildal, N. Soto, N. Gimelshein, N. Cone, N. Staudacher, N. Summers, N. LaFontaine, N. Chowdhury, N. Ryder, N. Stathas, N. Turley, N. Tezak, N. Felix, N. Kudige, N. Keskar, N. Deutsch, N. Bundick, N. Puckett, O. Nachum, O. Okelola, O. Boiko, O. Murk, O. Jaffe, O. Watkins, O. Godement, O. Campbell-Moore, P. Chao, P. McMillan, P. Belov, P. Su, P. Bak, P. Bakkum, P. Deng, P. Dolan, P. Hoeschele, P. Welinder, P. Tillet, P. Pronin, P. Tillet, P. Dhariwal, Q. Yuan, R. Dias, R. Lim, R. Arora, R. Troll, R. Lin, R. G. Lopes, R. Puri, R. Miyara, R. Leike, R. Gaubert, R. Zamani, R. Wang, R. Donnelly, R. Honsby, R. Smith, R. Sahai, R. Ramchandani, R. Huet, R. Carmichael, R. Zellers, R. Chen, R. Chen, R. Nigmatullin, R. Cheu, S. Jain, S. Altman, S. Schoenholz, S. Toizer, S. Miserendino, S. Agarwal, S. Culver, S. Ethersmith, S. Gray, S. Grove, S. Metzger, S. Hermani, S. Jain, S. Zhao, S. Wu, S. Jomoto, S. Wu, Shuaiqi, Xia, S. Phene, S. Papay, S. Narayanan, S. Coffey, S. Lee, S. Hall, S. Balaji, T. Broda, T. Stramer, T. Xu, T. Gogineni, T. Christianson, T. Sanders, T. Patwardhan, T. Cunningham, T. Degry,

- T. Dimson, T. Raoux, T. Shadwell, T. Zheng, T. Underwood, T. Markov, T. Sherbakov, T. Rubin, T. Stasi, T. Kaftan, T. Heywood, T. Peterson, T. Walters, T. Eloundou, V. Qi, V. Moeller, V. Monaco, V. Kuo, V. Fomenko, W. Chang, W. Zheng, W. Zhou, W. Manassra, W. Sheu, W. Zaremba, Y. Patil, Y. Qian, Y. Kim, Y. Cheng, Y. Zhang, Y. He, Y. Zhang, Y. Jin, Y. Dai, and Y. Malkov. Gpt-4o system card, 2024. URL <https://arxiv.org/abs/2410.21276>.
- [54] N. Ravi, V. Gabeur, Y.-T. Hu, R. Hu, C. Ryali, T. Ma, H. Khedr, R. Rädle, C. Rolland, L. Gustafson, E. Mintun, J. Pan, K. V. Alwala, N. Carion, C.-Y. Wu, R. Girshick, P. Dollár, and C. Feichtenhofer. Sam 2: Segment anything in images and videos. *arXiv preprint arXiv:2408.00714*, 2024. URL <https://arxiv.org/abs/2408.00714>.
- [55] S. Liu, Z. Zeng, T. Ren, F. Li, H. Zhang, J. Yang, C. Li, J. Yang, H. Su, J. Zhu, et al. Grounding dino: Marrying dino with grounded pre-training for open-set object detection. *arXiv preprint arXiv:2303.05499*, 2023.
- [56] W. Yuan, B. Eckart, K. Kim, V. Jampani, D. Fox, and J. Kautz. Deepgmr: Learning latent gaussian mixture models for registration. In *European Conference on Computer Vision*, pages 733–750. Springer, 2020.

A Appendix

A.1 PRISM Scene Generation

PRISM consists of 100k views of 10k scenes, generated via procedural generation of 2,365 object instances across 91 object classes, enumerated in Table 3. Procedural scene composition allows us to generate a wide variety of scenes at scale, maximizing both data diversity and quantity. We employ aggressive randomization in this process, the bounds for which are outlined in Table 2.

To evaluate a model’s ability to perform task-oriented grasping on new scenes, we create PRISM-Test, composed of novel object instances and classes. Specifically, we hold out 10% (rounded up) of object instances from each object class, and also 4 entire object classes (TeaCup, Fork, DSLRCamera, and PillBottle). This not only ensures that models do not overfit to the objects seen during training, but also tests their ability to generalize grasping to completely novel objects.

A.2 Grasp Sampling

The ACRONYM dataset provides roughly 2,000 grasps on each object mesh in the dataset, about half of which are labeled as stable grasps. Since we aim to collect object-grasp descriptions, it would be prohibitively expensive to do so for every grasp in the ACRONYM dataset. To alleviate this, we sample a subset of grasps for each object mesh for labeling. In practice, we sample 4 grasps per object mesh.

Standard practice for subsampling would be to use farthest-point sampling, i.e. per-instance grasp sampling. However, we see that doing so for each object mesh independently tends to create clusters of grasps, instead of creating a uniform distribution of grasps over the object. This is largely due to the fact that objects of the same class tend to have similar morphologies, and therefore have certain parts that are closer to or further from each other. This results in farthest point sampling picking grasps on similar parts for every object instance in a class, reducing the diversity of grasps on a type of object.

To counteract this, we introduce cross-instance grasp sampling, visualized in Figure 5. Concretely, within a class, we sample grasps on an object instance while considering grasps on similar parts of different object instances. This can be achieved by aligning object meshes within a class to each other, which we do as follows. We first notice that since the up-vector is known for all objects

Min. distance from table to wall (m)	2
Room dimensions (m×m)	[4, 10] × [4, 10]
Camera DFOV (deg)	[60, 110]
Camera distance (m)	[0.25, 1.25]
Camera pitch perturbation (frac. of VFOV)	[0, 0.02]
Camera yaw perturbation (frac. of HFOV)	[0, 0.05]
Camera roll perturbation (rad)	[0, 0.39]
Camera elevation (rad)	[$\pi/8$, $\pi/3$]
Image size (px)	480 × 640
Number of views per scene	10
Min. # of annotations per view	2
Number of objects	[6, 12]
Max. grasp distance (m)	1.0
Color temperature (K)	[2000, 10000]
Light intensity (lux)	[10, 25]
Light azimuth (rad)	[0, 2π]
Light inclination (rad)	[0, $\pi/3$]

Table 2: The randomization parameters used for scene generation in PRISM.

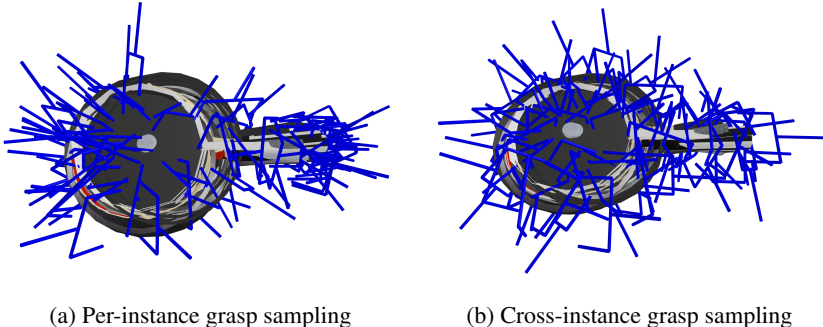


Figure 5: Cross-instance grasp sampling (right) creates a subset of grasps with much better coverage and diversity than independent per-instance grasp sampling (left).

meshes, we need only to align the object meshes in the xy-plane. We first project the mesh to the xy-plane, and sample 1000 points within the resulting polygon. We then align the centroids of these sets of points, and align orientations using the principal axes. We finally refine with iterative closest point (ICP) to retrieve a transform, which we apply to the object mesh.

After aligning meshes within a class, we use farthest point sampling in a round-robin fashion, sampling the furthest grasp for each object instance until we get 4 grasps per instance. For any object meshes for which this registration process fails, we use farthest point sampling independent of the other meshes.

A.3 Grasp Description Generation

In Section 3.1, we outline how we use GPT-4o to generate synthetic grasp descriptions. We illustrate an example of this process in Figure 6. Since GPT-4o can hallucinate incorrect spatial relations or grounding, we ask Prolific workers to manually verify the generated descriptions, and provide corrections if necessary. Full prompts are given in Figure 9.

A.4 Task Generation

We provide more details about the two steps involved in semantic grasping task generation (Task Generation paragraph in Section 3.1).

For the **grasp description generation** step, the structure of the required response is made to facilitate a causal explanation of the choices made while discouraging hallucinations. First, the LLM generates a list of object subtypes and identifies a list of optional parts only present in some subtypes, followed by a list of common object parts for any object of the given type (and subtypes). We then let the LLM assume a relative starting pose of the object relative to the supporting surface and describe it as the object parts in contact with the surface. The LLM then generates a list of

banana, bag, beer bottle, book, bottle, bowl, bread slice, calculator, camera, candle, canister, can opener, cap, carrot, cassette, cell phone, cereal box, chocolate, coaster, coin, computer mouse, controller, cookie, cup, cup cake, desk lamp, disc case, donut, drink bottle, drinking utensil, DSLR camera, eraser, flashlight, food item, fork, fruit, glasses, guitar, hammer, hanger, hat, headphones, keyboard, knife, laptop, magnet, marker, media discs, milk carton, mouse pad, mug, Nintendo DS, notepad, pan, paper box, paper clip, pen, pencil, picture frame, pill bottle, plate, power strip, purse, radio, ring, Rubik’s cube, ruler, scissors, screw driver, shampoo, shoes, soap bar, soap bottle, soda can, spoon, stapler, table clock, table lamp, tape measure, teacup, teapot, toilet paper, USB stick, video game controller, wall clock, wallet, watch, web cam, Wii, wine bottle, and wine glass

Table 3: The 91 **object classes** corresponding to the 2,365 objects included in PRISM.

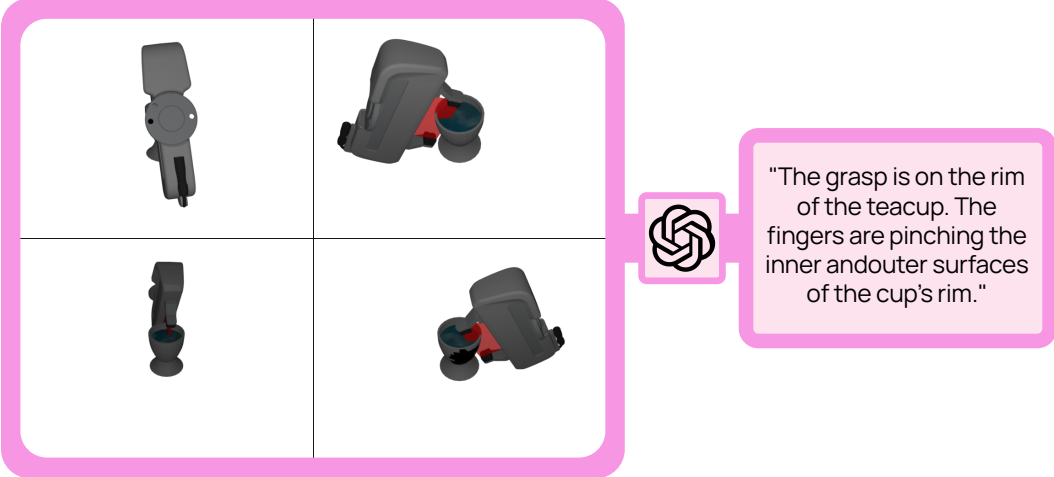


Figure 6: Given multiple views of a grasp on an object mesh, GPT-4o describes the grasp in natural language. The red rectangle rendered in the collage helps the VLM to understand the volume grasped by the gripper, and how it intersects the object mesh.

common graspable parts, excluding optional parts, and the target list of grasp descriptors. Each grasp is generated as (1) the object part to contact, (2) an example semantic task, (3) an approach direction, finger-plane and gripper orientation, which provide redundancy to discourage inconsistent or implausible grasps, and (4) a natural language description of the grasp (excluding any reference to the example task). The prompt in use is shown in Figure 10.

For the **semantic manipulation task generation** step we ask the LLM to generate four valid semantic tasks per grasp conditioned on the object class, its relative starting pose, and the target and alternative grasp descriptions (excluding the example semantic tasks used to guide grasp generation). Each semantic task is generated as (1) the task instruction in natural language (avoiding any reference to the grasp), complemented with the number of grippers required to complete the task beyond the initial grasp, (2) a grasp critique seeking possible unsuitability of the grasp for the task and a grasp score in the range 0 (worst validity) to 9 (best), (3) an alternative grasp critique seeking possible suitability of the alternative grasp and corresponding grasp score, and (4) an analysis of the validity of the task definition, considering lack of assumptions about the object’s state and context, or physical plausibility of the grasp and task, among others, and a corresponding validity score, also in the range 0 to 9. The prompt in use is shown in Figure 11.

A.5 Grasp Matching

In Section 3.1, we outline how generated possible tasks and grasps that would accomplish those tasks for each object, and then match those grasp descriptions with those from the ACRONYM dataset using GPT-4o. We illustrate sample matched tasks and grasps in Figure 7 and give the system and user prompts for this process in Figure 12.

A.6 TaskGrasp-Image Registration

In Section 3.2 we describe how the TaskGrasp-Image benchmark preserves the ground-truth annotations of TaskGrasp, while eliminating noise and artifacts by placing them in the context of real-world images. We now describe how we derive TaskGrasp-Image.

Recall that TaskGrasp fuses multiple RGB-D observations to create a segmented point cloud, which is used for grasp annotation. TaskGrasp-Image is created by transforming these annotated grasps back into each captured image frame. Unfortunately, the transformation between the point cloud



Gently press down on the bag's main body to flatten it against the surface.



Lift the bag off the surface and swing it gently forward, as to set it onto a nearby bench.



Feed the power strip's cord into a cord management clip affixed to the side of the table.



Flip the power strip over to inspect the information printed on its underside.

Figure 7: Representative grasp annotations from PRISM, consisting of a grasp on an object with a corresponding task instruction. Note how different tasks require different grasps on the same object.

and the RGB-D views were not published, but we can recover them using pointcloud registration techniques.

First, for each image we use GroundingDINO [55] and SAM2 [54] to segment out the object mask. Using the depth map, we then backproject a partial 3D point cloud of the object, which we can register with the fused object point cloud. To do so, we first use DeepGMR [56] to roughly align the point clouds, and then refine using iterative closest point (ICP). Finally, we reject failed registrations by rejecting any with a final residual error exceeding 0.006. This results in 299 successfully registered views.

Now that we have recovered the transform between the fused point clouds and the original RGB-D views, we transform the annotated grasps from the point cloud into the camera frame of each viewpoint. We visualize an representative result of this process in Figure 8.

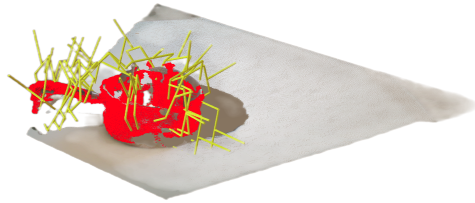


Figure 8: A visualization of the segmented pointcloud (red) of a pot registered to one of the input RGB-D views. By performing this registration, we can transform the annotated grasps (yellow) into the camera frame.

A.7 Training GraspMolmo

In Section 3.3 we outline the training process for GraspMolmo, which largely follows from [15]. Our training data mixture is mostly the same, with PRISM-Train and TaskGrasp-Image added, and the original data proportionally downweighted. The complete mixture is outlined in Table 4. We start with the Molmo-7B-D-0924 model and finetune on this data for 10,000 steps with a batch size per device of 8, on 64 Nvidia H100 GPUs, taking approximately 9 hours.

45%	PRISM-Train
10%	TaskGrasp-Image (split t/0)
	PixMo-AskModelAnything
15%	PixMo-Cap
	PixMo-CapQA
	PixMo-Point-Explanations
20%	PixMo-Points
	PixMo-Count
10%	VQA v2.0 (COCO 2014 subset), TextVQA, OK-VQA, ChartQA, DocVQA, InfographicVQA, AI2D, A-OKVQA, AndroidControl, ScienceQA, TabMWP, ST-VQA, TallyQA, DVQA, FigureQA, PlotQA, PixMo-Clocks

Table 4: Training data mixture for GraspMolmo.

A.8 Real-Robot Evaluation

In Section 4 we test multiple TOG models on multiple challenging semantic grasping tasks in realistic cluttered scenes. We enumerate the manipulated objects and the associated tasks in Table 5. Notably, we select the tasks such that the robot must grasp the object in different ways. This ensures that we test a model’s ability to understand task-level semantics (where to grasp an object for a particular task) rather than simply memorizing object-level semantics (where to grasp an object independent of task).

	French Press	“Pour coffee from the french press” “Press down the knob of the plunger of the french press”
Scene 1	Kitchen Knife	“Use the knife to cut fruit” “Hand me the knife safely”
	Mug	“Pour the water out of the blue mug” “Hang the blue mug onto a hook by the handle”
Scene 2	Water Bottle	“Open the lid of the water bottle” “Give me some water”
	Sink	“Adjust the faucet” “Turn on the sink”
Scene 3	Spray Bottle	“Spray cleaning solution with the spray bottle” “Unscrew the spray bottle”
	Books	“Pass the book written by Greg Bear” “Pass the book written by Orson Scott Card”
Scene 3	Telephone	“Answer the phone” “Put the phone back on the hook ”
	Flower + Vase	“Take the flowers out of the vase” “Dump the flowers out of the vase”

Table 5: We evaluate on a variety of **real-world objects in multiple scenes** representative of in-home use cases. For each object, we test multiple tasks which require different grasping affordances.

SYSTEM PROMPT:

You are an expert in robotic grasp analysis. Your task is to generate precise and concise descriptions of robotic grasps in images. Each image contains a robotic gripper interacting with an object. A red rectangle marks the area between the fingers of the gripper, which helps you identify the grasp location. Your goal is to describe where the gripper is grasping the object and what the fingers are pinching. Follow these guidelines:

- Clearly specify the grasp location on the object (e.g., “on the handle”, “near the rim”, “on the body”, “at the base”).
- Indicate how the fingers of the gripper interact with the object (e.g., “gripping the inner and outer surfaces,” “pinching from opposite sides”).
- The image may contain multiple viewpoints, but your description should focus on the grasp itself rather than commenting on different perspectives.
- Do not speculate about grasp stability or effectiveness.
- Keep the description concise but detailed, focusing only on the grasp.
- Do not mention the red rectangle in your description, it is only for visualization.

Example of a good description:

“The grasp is on the rim of the pan, approximately opposite the handle.
The fingers are gripping the inside and outside of the pan’s rim.”

Your response should always describe the grasp clearly and concisely without asking for additional input.

USER PROMPT:

These are multiple views of a(n) <object_name>. Describe the grasp.

Figure 9: System and user prompt used with GPT-4o to generate synthetic grasp descriptions for grasps in the ACRONYM dataset.

For objects of a given category, we need to determine two grasp definitions considering a single 6-DOF end effector that are as varied as possible (e.g., for ladles we would probably define one grasp around the handle and another one around the bowl, possibly requiring different relative orientations of the gripper with respect to the object part) and are reasonable for specific tasks/contexts (think about different grasps when using, cleaning, or handing a knife). Assuming that the objects from each category are standing or lying on a table or similar surface, avoid grasps that assume that the object needs to be approached from underneath or example tasks that require the object to be placed upright while holding it from underneath for the target object pose on some surface. Do not assume the presence of any optional feature in an object of the given category (e.g. some chair subtypes might have legs, but others a wheeled base instead, while all chairs have a back rest and a seat). Related, if the object category is too generic to identify object parts (e.g. an undetermined ‘tool’), feel free to return an empty list. Generate the output as a JSON dict with:

- ‘object_subtypes’ (list of str, possibly empty) different types of object for the given category (which might include specific optional parts),
- ‘optional_parts’ (list of str, possibly empty) present in only some objects of the category and subtypes and should be avoided
- ‘common_parts’ (list of str, possibly empty) reasonably comprehensive list of parts of any object of the given category (no optional ones). Here you can merge parts that might be differently named in subclasses but offer a common affordance for any object of the category or subtype(s)
- ‘object_table_contact_parts’ (list of str) part(s) of object that are assumed to be in contact with the table or surface underneath in the default starting pose (this defines a starting object orientation). If more than one part, make sure these are plausibly simultaneously in contact with the underlying surface,
- ‘common_graspable_parts’ (list of str, possibly empty) that can be used to generate grasps for any object of the category
- ‘grasps’, a list of two dicts with the entries:
 - ‘object_part’ (str),
 - ‘example_task’(str),
 - ‘approach_direction’ (str, for wrist axis, e.g. from above, from the side, from below, at an angle, if relevant, else ‘Any’, relative to the orientation implied by the object-table contact parts),
 - ‘finger_plane’ (str, relative to wrist axis, e.g. left/right or up/down relative to the arm’s axis, if relevant, else ‘Any’),
 - ‘gripper_orientation’ (str, whether the gripper faces up, down, sideways, or is diagonal/angled tilted, if relevant, else ‘Any’),
 - ‘natural_language’ (str, description of the grasp in natural language, avoiding any reference to the example task and avoiding irrelevant grasp parameters, if any)

Make sure that example tasks do not state the object part to contact or the direction to approach, and are unfeasible for the alternative grasp(s) in the list. If these requirements seem impossible to fulfill, it is best to return an empty list of grasps. Be very descriptive about the relative gripper orientations.

One example for the ‘drill’ category would be:
 [DRILL ANNOTATION EXAMPLE]

Feel free to discuss options to annotate the object type while fulfilling the requirements before generating the JSON dict. The object type to annotate is [CATEGORY].

Figure 10: **Prompt template for grasp description** used in the first step of task generation.

We need to generate semantic manipulation tasks requiring each of the given grasps in the list provided at the end. Please generate the tasks for each grasp with the following design criteria, where each criterion is first identified by a short name and then described in more detail:

1. Clear target. Ensure that every task mentions the object type (e.g., 'the mug') unless it is obvious without it.
2. Unknown state. Avoid tasks that make assumptions about the state of the object (e.g. being open/closed, empty/full, etc.).
3. Unknown context. Avoid tasks that make assumptions about the surroundings/context of the object (i.e. assuming the presence of any other objects of the same category or others in the scene, other than the presence of a table top or similar surface underneath the object at the start).
4. Implicit grasp. Avoid references to the part of the object being grasped (e.g., 'by the handle') or any of the grasp definition parameters in the task definition.
5. Single gripper. While you should favor single-gripper task definitions, if a second gripper is implied or required, it should not be assumed to be present for the initial grasp, but rather during a subsequent step (e.g. if 'while another gripper does ...' seems reasonable, convert it into 'for posterior...').
6. Physical plausibility. Avoid tasks that require physically implausible configurations, like the object being placed standing on some surface while held from underneath.
7. Compact instruction. Write tasks in compact and intelligible natural language and avoid technical formating like snake case.
8. Semantic meaning. Avoid simple pick and place tasks, and try to focus on semantic tasks, i.e., they should rely on some affordance of the object or consider some compositional task where we must manipulate the object towards some meaningful goal.
9. Identifiability. If both provided grasps, object category or parts to grasp seem too coarse/vague/hard to identify, avoid defining any task and favor an empty list of tasks for each grasp.

Try to generate four valid semantic tasks per grasp, making sure that the tasks are incompatible with the alternative grasp for the object category (they should imply different use cases or affordances). For each generated semantic task we need a dict with the entries:

- 'text': the semantic task instruction, without mentioning the grasped part or approach direction, and mentioning the target object if needed,
- 'num_grippers': the number of grippers required to complete the semantic task,
- 'grasp_critique': short string justifying the lack of validity of the assigned grasp towards completing the task,
- 'grasp_score': validity score in range 0 (low) to 9 (high) based on the grasp_critique,
- 'alternative_grasp_critique': short string justifying the possible validity of the alternative grasp towards completing the task,
- 'alternative_grasp_score': validity score in range 0 to 9 according based on the alternative_grasp_critique,
- 'weakest_point': short name (string) of the task design criterion point most poorly fulfilled,
- 'task_criteria_fulfilled': score the fulfillment of the weakest point in the range 0 (poor) to 9 (perfect fulfillment)

Feel free to reason about the problem and generate a JSON dictionary mapping each grasp id to the list of semantic task dicts.

The following are the valid grasp ids and corresponding info for an object of type '[CATEGORY]' assuming the object is in contact with the underlying surface through its part(s) [OBJECT SURFACE CONTACTS]:
[GRASP INFOS WITHOUT EXAMPLE TASKS]

Figure 11: **Prompt template for semantic task generation**, used in the second step.

SYSTEM PROMPT:

You are a linguistic and robotic expert. You are tasked with matching a candidate grasp description to one or more of multiple options, called annotated grasp descriptions.

You will be given a candidate grasp description, which is a description of how a robot could grasp a specific object. You will also be given a list of annotated grasp descriptions, which are multiple known descriptions of how a robot could grasp the same object. You should choose the annotated grasp descriptions that have the same meaning as the candidate grasp description. In this case, "meaning" means that the candidate grasp description and the annotated grasp description describe a grasp on a similar part of the object, in a similar manner.

For example, if the candidate grasp description is "grasp the midpoint of the handle of the mug", and one of the annotated grasp descriptions is "grasp the handle of the mug", then you should choose that annotated grasp description. If there are multiple annotated grasp descriptions that have the same meaning as the candidate grasp description, you should return all of them. If there are no suitably matching annotated grasp descriptions, you should return an empty list.

You should output a JSON object with the following fields:

- candidate_grasp_desc: the candidate grasp description which you are prompted with
- matching_grasp_descs: a list of annotated grasp descriptions that have the same meaning as the candidate grasp description

USER PROMPT:

The object is a(n) <object_category>. The candidate grasp description is: "<candidate_grasp>". The annotated grasp descriptions are:

- <grasp_description_1>
- <grasp_description_2>
- ...

Figure 12: System and user prompt used with GPT-4o to match generated candidate grasp descriptions with synthetically generated descriptions of ACRONYM grasps.